

Chemical transport model ozone simulations for spring 2001 over the western Pacific: Regional ozone production and its global impacts

Oliver Wild,¹ Michael J. Prather,² Hajime Akimoto,¹ Jostein K. Sundet,³ Ivar S. A. Isaksen,³ James H. Crawford,⁴ Douglas D. Davis,⁵ Melody A. Avery,⁴ Yutaka Kondo,⁶ Glen W. Sachse,⁴ and Scott T. Sandholm⁵

Received 4 August 2003; revised 24 October 2003; accepted 6 November 2003; published 21 May 2004.

[1] The spatial and temporal variation in ozone production over major source regions in East Asia during the NASA Transport and Chemical Evolution over the Pacific (TRACE-P) measurement campaign in spring 2001 is assessed using a global chemical transport model. There is a strong latitudinal gradient in ozone production in springtime, driven by regional photochemistry, which rapidly diminishes as the season progresses. The great variability in meteorological conditions characteristic of East Asia in springtime leads to large daily variability in regional ozone formation, but we find that it has relatively little impact on the total global production. We note that transport processes effectively modulate and thus stabilize total ozone production through their influence over its location. However, the impact on the global ozone burden, important for assessing the effects of precursor emissions on tropospheric oxidizing capacity and climate, is sensitive to local meteorology through the effects of location on chemical lifetime. Stagnant, anticyclonic conditions conducive to substantial boundary layer ozone production typically allow little lifting of precursors into the free troposphere where greater ozone production could occur, and the consequent shorter chemical lifetime for ozone leads to relatively small impacts on global ozone. Conversely, cyclonic conditions with heavy cloud cover suppressing regional ozone production are often associated with substantial cloud convection, enhancing subsequent production in the free troposphere where chemical lifetimes are longer, and the impacts on global ozone are correspondingly greater. We find that ozone formation in the boundary layer and free troposphere outside the region of precursor emissions dominates total gross production from these sources in springtime, and that it makes a big contribution to the long range transport of ozone, which is greatest in this season. **INDEX TERMS:** 0345 Atmospheric Composition and Structure: Pollution—urban and regional (0305); 0365 Atmospheric Composition and Structure: Troposphere—composition and chemistry; 0368 Atmospheric Composition and Structure: Troposphere—constituent transport and chemistry; **KEYWORDS:** tropospheric ozone, western Pacific, meteorological variability

Citation: Wild, O., et al. (2004), Chemical transport model ozone simulations for spring 2001 over the western Pacific: Regional ozone production and its global impacts, *J. Geophys. Res.*, 109, D15S02, doi:10.1029/2003JD004041.

1. Introduction

[2] Photochemical formation of ozone in the troposphere from precursor species such as nitrogen oxides (NO_x),

carbon monoxide (CO) and hydrocarbons leads to a degradation of local air quality [Haagen-Smit, 1952] and to a global increase in O₃ that leads to a global warming [Lacis et al., 1990; Hansen et al., 1997]. The link between these regional and global impacts is becoming increasingly evident [Hansen, 2002]. Ozone is also the principal source of tropospheric OH radicals and therefore controls the rate at which gases such as methane are oxidized [e.g., Chameides and Walker, 1973; Crutzen, 1974; Thompson, 1992]. On a global scale, the photochemical production of O₃ in the troposphere generally dominates the stratospheric influx [Liu et al., 1980; Lelieveld and Dentener, 2000; Prather and Ehhalt, 2001]. While the production mechanisms are well known [e.g., Chameides and Walker, 1973; Crutzen, 1974; Logan et al., 1981], the magnitude, timing and

¹Frontier Research System for Global Change, Yokohama, Japan.

²Earth System Science, University of California, Irvine, California, USA.

³Department of Geophysics, University of Oslo, Oslo, Norway.

⁴NASA Langley Research Center, Hampton, Virginia, USA.

⁵School of Earth and Atmospheric Sciences, Georgia Institute of Technology, Atlanta, Georgia, USA.

⁶Research Center for Advanced Science and Technology, University of Tokyo, Japan.

location of greatest O₃ formation depend on the meteorological environment about the region of precursor emissions. Meteorological processes effectively modulate the chemical processing of O₃ through the amount of sunlight and water vapor, the residence time in the boundary layer, the dilution and mixing of different precursors and their scavenging by clouds and precipitation, and the long-range transport and dispersion of the O₃ produced.

[3] In the polluted boundary layer, the lifetime of O₃ to chemical destruction and deposition is relatively short (days), but it remains longer than typical dynamical time scales (hours to days), and hence much of the O₃ formed may be transported to cleaner environments. Atmospheric lifting processes associated with convection or frontal systems [Pickering *et al.*, 1990; Bethan *et al.*, 1998] are particularly important in controlling the global impacts of the O₃ formed as they raise it higher into the troposphere where the lifetime to chemical destruction is longer (weeks to months). Transport of O₃ precursors out of polluted emission regions typically leads to slower but greater total O₃ production [Liu *et al.*, 1987], and supplements production from sources in the troposphere such as lightning. The export of short-lived precursors such as NO_x is generally inefficient [Horowitz *et al.*, 1998] and subsequent O₃ production in the free troposphere from boundary layer sources is therefore dependent on temporary storage as longer-lived NO_y species and on the location and timing of rapid vertical transport by convection. Chatfield and Delany [1990] provided contrasting examples of O₃ production in biomass burning plumes undergoing delayed or immediate convective lifting, colorfully termed “cook-then-mix” and “mix-then-cook” scenarios, demonstrating very different impacts on regional and global O₃. While rapid boundary layer formation in stagnant conditions over polluted urban regions in the presence of strong sunlight and high temperatures may lead to a large buildup of smog O₃, Sillman and Samson [1995] speculated that the impacts on global O₃, and hence on climate, may be less than in overcast conditions where O₃ buildup is small, but the export of precursors is larger. The balance between regional and downwind production and its sensitivity to meteorology is thus important both for assessing the impacts of surface emissions on air quality and climate, and for understanding how global or regional climate change may affect these impacts in the future.

[4] This study uses the extensive set of measurements and analysis from the NASA Transport and Chemical Evolution over the Pacific (TRACE-P) measurement campaign held in spring 2001 [Jacob *et al.*, 2003] as a case study to examine the meteorological factors controlling production of O₃ from fossil fuel sources over East Asia. Outflow of pollution from rapidly developing countries around the Pacific Rim is known to influence tropospheric O₃ on a hemispheric scale, and has the greatest effects in springtime [Berntsen *et al.*, 1996; Jacob *et al.*, 1999; Mauzerall *et al.*, 2000; Wild and Akimoto, 2001; Bey *et al.*, 2001]. The meteorology of the region in spring is characterized by strong frontal activity which lifts pollution into the path of strong westerly winds which may carry it across the Pacific. This transport is consequently episodic in nature [Yienger *et al.*, 2000], as the passage of successive low pressure systems interlaces polluted continental outflow with cleaner, marine air and

with dry air from the stratosphere descending in trailing anticyclones [Carmichael *et al.*, 1998]. The meteorological processes leading to this variability in outflow also strongly influence O₃ production directly via their impacts on mixing processes, humidity, photolysis rates and scavenging of precursors, providing ideal conditions for study of variability in O₃ production and its global impacts.

[5] While previous studies have characterized the production and export of O₃ from East Asia on a seasonal or annual basis, this study uses the day-to-day variations in weather to identify the meteorological factors controlling the buildup of tropospheric O₃. By following the emission of O₃ precursors each day from a specified region independently, we show how the different meteorological conditions affect local versus regional production and thus how the synoptic weather patterns control the net impact of emissions on global tropospheric O₃. The principal aims of the paper are to quantify the contributions of East Asian emissions to global O₃ during springtime, to relate these to the meteorological conditions over the source region, and thus to examine how meteorological mechanisms control the balance between local air quality and global climate forcing.

[6] In section 2, we evaluate the performance of the model used in this study against O₃ tendencies derived from TRACE-P observations. This campaign provided extensive observational data from two aircraft operating in the region with sufficient detail to allow thorough testing of current photochemical theory [Cantrell *et al.*, 2003]. We examine the regional production of O₃ from East Asia during the spring of 2001 in section 3. We then focus on the daily variability in O₃ production from each day's emissions in section 4, exploring its dependence on meteorological conditions, and noting generally opposite impacts on air quality and climate forcing. We conclude by testing the sensitivity of production to specific meteorological variables, and identifying potential biases in this study.

2. Chemical Transport Model Ozone Production

[7] This study uses the Frontier Research System for Global Change (FRSGC) version of the University of California, Irvine (UCI), global chemical transport model (CTM), described by Wild and Prather [2000]. The model is run at T63 resolution (1.9° × 1.9°), with 37 eta levels in the vertical, and is driven by 3-hour meteorological fields for spring 2001 generated with the European Centre for Medium-Range Weather Forecasts (ECMWF) Integrated Forecast System (IFS). The configuration of the model and meteorological data used in these studies is described in more detail by Wild *et al.* [2003] and is presented with an evaluation of the O₃ simulation during the TRACE-P period against observations from aircraft, ozonesondes, and satellite. The model uses a linearized stratospheric chemistry for O₃ [McLinden *et al.*, 2000] and calculates a reasonable net flux of O₃ from the stratosphere to the troposphere of 557 Tg yr⁻¹. With this treatment, the model is able to capture the short-term variations in total column O₃ which affect photolysis rates in the troposphere, as well as the magnitude and timing of stratospheric intrusions [Wild *et al.*, 2003]. The general features of the O₃ distribution over

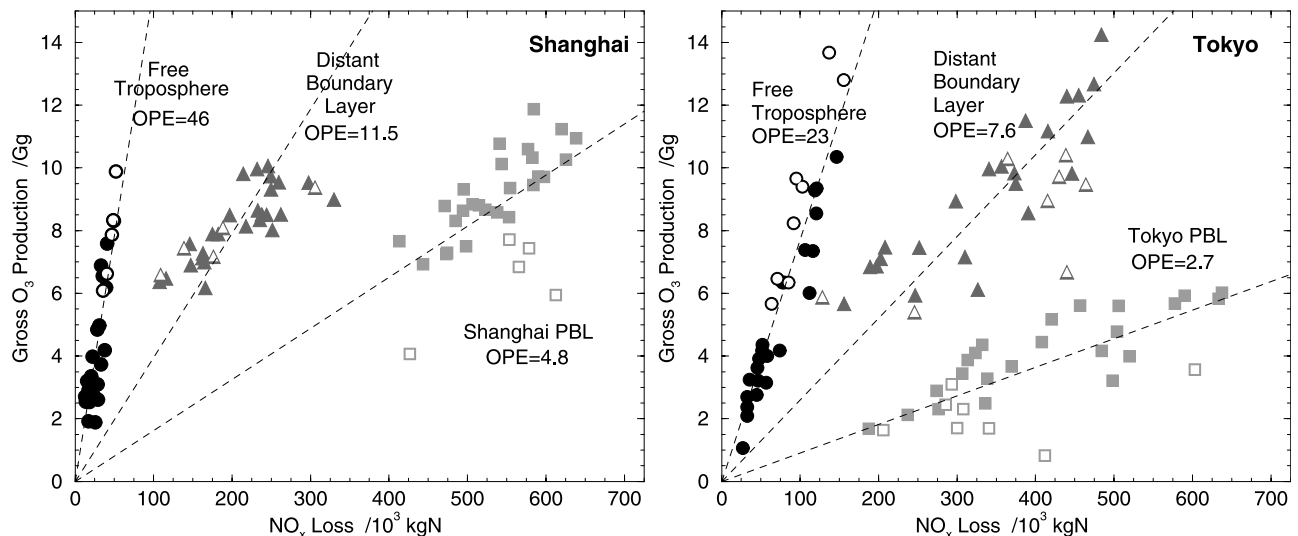


Figure 10. Gross production of O_3 and loss of NO_x from 1 day of emissions over (left) Shanghai and (right) Tokyo for each day of March showing formation in the regional boundary layer (squares), in the distant boundary layer (triangles) and in the free troposphere (circles). Open symbols indicate days with heavy daytime cloud cover. See color version of this figure in the HTML.

values are sufficiently different over the domains considered, typically a factor of 10 between the polluted boundary layer and the free troposphere, that the clusters remain quite distinct. Comparing the mean O_3 production and NO_x loss over each domain we find that about 40% of the gross O_3 production over Shanghai occurs in the boundary layer from about 70% of the NO_x emitted. Respectively 40% and 20% of the production occur in the distant boundary layer and free troposphere, where production efficiencies are higher. Chemical timescales are sufficiently rapid that the boundary layer dominates removal of NO_x , and only an average of 4% reaches the free troposphere. Note, however, that the coarse model resolution used in these simulations may lead to a systematic bias in these conditions, with an underestimation of NO_x export as seen in section 2. Over Tokyo, 20% of the production occurs in the boundary layer from 50% of the NO_x emitted, with another 50% in the boundary layer outside the source region. Slower chemical production and shorter dynamical timescales lead to a much greater variability in boundary layer NO_x removal, and an average of 10% reaches the free troposphere. The O_3 production efficiencies over each domain are about half those over Shanghai, consistent with slower photochemical formation. However, the total production is similar due to the different distribution of production between the domains. This emphasizes the important role that transport of precursors plays in controlling gross O_3 production.

[32] Days with heavy daytime cloud cover (optical depth greater than 10) are highlighted with unfilled markers in Figure 10. These typically have lower production efficiencies in the regional boundary layer due to the increased cloud cover, but slightly higher production efficiencies in the free troposphere. Boundary layer NO_x loss is less than average due to the lower abundance of OH, and a greater proportion of the NO_x is lifted into the troposphere by convective processes, where total production is about a

factor of two greater. Consequently, these changes in timescales shift some O_3 production out of the boundary layer into the free troposphere, but do not alter the gross production or the mean burden greatly. Comparing the 5 days of heavy cloud cover over Shanghai with 10 largely cloud-free days, we find an increase in gross production of 5% and an increase in mean burden of 10%, suggesting that the impact on global O_3 may be larger on overcast days than in fair-weather conditions.

4.5. Sensitivity to Meteorology

[33] To investigate the sensitivity of regional and global O_3 production to meteorological processes, we consider the changes to the conditions over Shanghai on 16 March required to reproduce the additional O_3 found on 12 March. Convection, rainfall and cloud optical depth over Shanghai are removed for 16 March, and the temperature, humidity, boundary layer height and the O_3 column used in calculating photolysis rates are set to approximate the fair-weather values of 12 March for both emission pulse and control run. With all changes applied, global production is $\sim 15\%$ greater than on 12 March, reflecting the effects of differing transport patterns and residence times, which were not altered.

[34] By altering each variable in turn, and neglecting the coupling between them, we estimate that $\sim 60\%$ of the difference in regional production is due to cloud cover suppressing photolysis rates, 20% is accounted for by reduced dilution of precursors due to the lower boundary layer height, and 15% is due to suppressed convection preventing lifting of precursors. The remaining 5% is dominated by increased temperature, but also reflects reduced humidity and total O_3 column. Suppressing convection reduces the global production by about 20%, reflecting the greater production efficiency per molecule of NO_x in the free troposphere, but reduces the additional

- Wild, O., J. K. Sundet, M. J. Prather, I. S. A. Isaksen, H. Akimoto, E. V. Browell, and S. J. Oltmans (2003), CTM Ozone Simulations for Spring 2001 over the western Pacific: Comparisons with TRACE-P Lidar, ozonesondes and TOMS columns, *J. Geophys. Res.*, *108*(D21), 8826, doi:10.1029/2002JD003283.
- Yienger, J. J., M. K. Galanter, T. A. Holloway, M. J. Phadnis, S. K. Guttikunda, G. R. Carmichael, W. J. Moxim, and H. Levy II (2000), The episodic nature of air pollution transport from Asia to North America, *J. Geophys. Res.*, *105*, 26,931–26,945.
- H. Akimoto and O. Wild, Frontier Research System for Global Change, 3172-25 Showa-machi, Kanazawa-ku, Yokohama, Kanagawa 236-0001, Japan. (akimoto@jamstec.go.jp; oliver@jamstec.go.jp)
- M. A. Avery, J. H. Crawford, and G. W. Sachse, NASA Langley Research Center, Hampton, VA 23681, USA. (m.a.avery@larc.nasa.gov; j.h.crawford@larc.nasa.gov; g.w.sachse@larc.nasa.gov)
- D. D. Davis and S. T. Sandholm, School of Earth and Atmospheric Sciences, Georgia Institute of Technology, Atlanta, GA 30332, USA. (douglas.davis@eas.gatech.edu; scott.sandholm@eas.gatech.edu)
- I. S. A. Isaksen and J. K. Sundet, Department of Geophysics, University of Oslo, P.O. Box 1022, Blindern 0315, Oslo, Norway. (i.s.a.isaksen@geofysikk.uio.no; j.k.sundet@geofysikk.uio.no)
- Y. Kondo, Research Center for Advanced Science and Technology, University of Tokyo, 4-6-1 Komaba, Meguro-ku, Tokyo 153-8904, Japan. (kondo@atmos.rcast.u-tokyo.ac.jp)
- M. J. Prather, Earth System Science, University of California, Irvine, CA 92697-3100, USA. (mprather@uci.edu)

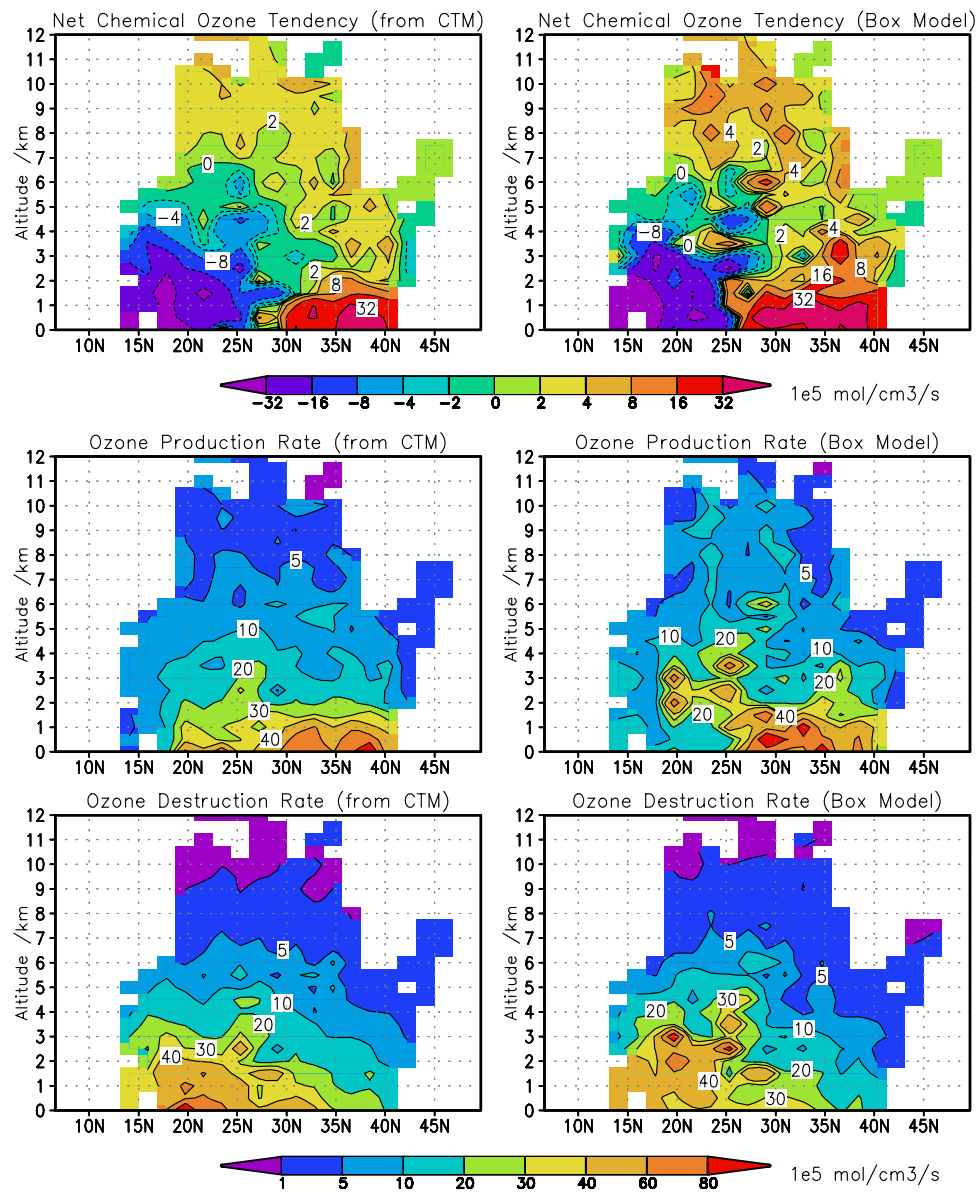


Figure 1. Net chemical O_3 tendency (10^5 molecules $cm^{-3} s^{-1}$, top) over the western Pacific (west of $145^\circ E$ south of $30^\circ N$, west of $160^\circ E$ north of $30^\circ N$) (left) from the CTM and (right) from steady state calculations constrained by aircraft measurements along flight tracks during the TRACE-P campaign. (bottom) Gross O_3 production and destruction rates. Note the different color scale used.

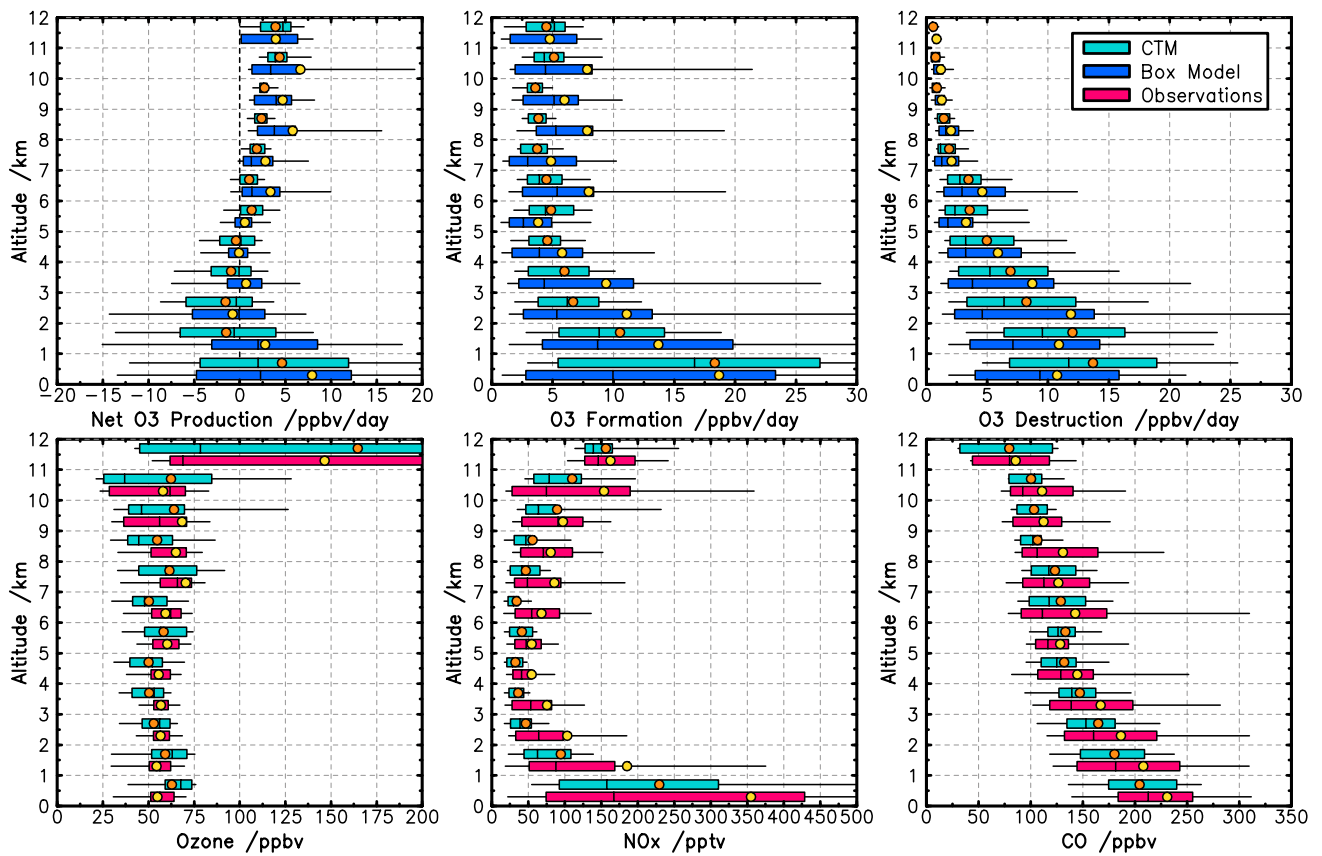


Figure 2. Profiles of sampled variables binned by altitude showing the mean (circles), median (vertical bar), quartiles (defining box) and 10th/90th percentiles (horizontal lines) at each 1-km level over the western Pacific region. CTM distributions are shown in cyan, aircraft observations in red, and instantaneous tendencies from steady state box model calculations in blue.